Acknowledgements

This work is supported by the Director, Office of Science, Office of Basic Energy Sciences, Materials Sciences Division, of the US Department of Energy at Lawrence Berkeley National Laboratory. P.G. and W.T. acknowledge support from the Deutsche Forschungsgemeinschaft.

Correspondence and requests for materials should be addressed to E.R. (e-mail: erotenberg@lbl.gov).

A DNA-fuelled molecular machine made of DNA

Bernard Yurke*, Andrew J. Turberfield*†, Allen P. Mills Jr*, Friedrich C. Simmel* & Jennifer L. Neumann*

** Bell Laboratories, Lucent Technologies, 600 Mountain Avenue, Murray Hill, New Jersey 07974, USA*
† Department of Physics, University of Oxford, Clarendon Laboratory, Parks Road, Oxford OX1 3PU, UK

Molecular recognition between complementary strands of DNA allows construction on a nanometre length scale. For example, DNA tags may be used to organize the assembly of colloidal particles[1,2], and DNA templates can direct the growth of semiconductor nanocrystals[3] and metal wires[4]. As a structural material in its own right, DNA can be used to make ordered static arrays of tiles[5], linked rings[6] and polyhedra[7]. The construction of active devices is also possible—for example, a nanomechanical switch[8], whose conformation is changed by inducing a transition in the chirality of the DNA double helix. Melting of chemically modified DNA has been induced by optical absorption[9], and conformational changes caused by the binding of oligonucleotides or other small groups have been shown to change the enzymatic activity of ribozymes[10–13]. Here we report the construction of a DNA machine in which the DNA is used not only as a structural material, but also as 'fuel'. The machine, made from three strands of DNA, has the form of a pair of tweezers. It may be closed and opened by addition of auxiliary strands of 'fuel' DNA; each cycle produces a duplex DNA waste product.

Single strands of DNA composed of complementary sequences of the bases adenine, cytosine, guanine and thymine (A, C, G and T) hybridize to form a stable duplex (double helix) bound together by hydrogen bonds between complementary base pairs (A–T and C–G). Our machine is prepared by mixing stoichiometric quantities of three strands, A, B and C, in SPSC buffer (see Methods) at 20 °C to give a final concentration of 1 μM; the base sequences chosen for the three strands are given in Fig. 1. The structure and operation of the machine are shown in Fig. 2. Strand A consists of two 18-base sequences which hybridize with complementary sequences at the ends of strands B and C to form two stiff[14] arms; the hinge is formed from a four-base single-stranded region of A between the regions hybridized to strands B and C. In the machine's rest state, the remaining unhybridized 24-base portions of the 42-base strands B and C dangle floppily from the ends of the tweezers: double-stranded DNA has a persistence length of the order of 100 base pairs[14,15], whereas at 1 M salt concentration single-stranded DNA has a persistence length of about 1 nm (ref. 16)—or approximately three bases.

Strand A is labelled at the 5′ and 3′ ends with dyes TET (5′ tetrachloro-fluorescein phosphoramidite) and TAMRA (carboxy-tetramethylrhodamine), respectively. When TET is excited by the 514.5-nm emission of an argon ion laser, it fluoresces with a peak emission wavelength of 536 nm; this emission is quenched by resonant intramolecular energy transfer from TET to TAMRA (a longer-wavelength dye whose absorption band overlaps the emission band of TET) with an efficiency that decreases rapidly as the distance between the dyes increases[17]. Fluorescence quenching is used as an indicator[18] to titrate strands B and C against A; as half of A is straightened from a random coil by hybridization with B (or C), the mean separation between the dye groups on A increases leading to a fivefold increase in the fluorescence intensity. The cumulative effect of hybridization with both B and C is a sevenfold increase in fluorescence intensity in the rest state.

The assembled tweezers are opened and closed with fuel strands F and $\bar{F}$. The 56-base closing strand F consists of two consecutive 24-base sections, which are complementary to the dangling ends of B and C, with an additional 8-base overhang section. Figure 2b shows how closing strand F hybridizes with the free ends of strands B and C, pulling the ends of the tweezers together. The average free-energy change associated with the hybridization of a complementary base pair is −78 meV (−1.8 kcal mol^{-1}) at 20 °C (ref. 19) and the separation between base pairs in single-stranded DNA is 0.43 nm (ref. 20), giving an average closing force of about 15 pN which is consistent with that required to pull apart double-stranded DNA[21]. This is at the upper end of the range of measured forces exerted by single-group kinesin[22,23] and myosin[24,25] motors. The second component of the fuel is removal strand $\bar{F}$, the complement of F: the additional free energy gained when the overhang (single-stranded in the initial state) hybridizes with $\bar{F}$ ensures that when a stoichiometric quantity of $\bar{F}$ is added it removes F from the machine to form a double-stranded waste product F$\bar{F}$ and returns the tweezers to the open state. Hybridization between the closing and removal fuel strands is expected to occur first at the exposed overhang[26] and to proceed by branch migration[27], a random walk of the junction between the region of F newly hybridized to the removal strand $\bar{F}$ and the region still hybridized to the tweezer components B and C; this branch migration continues until both B and C have been completely displaced and the F$\bar{F}$ duplex diffuses away. The random walk occurs sufficiently quickly that the rate-limiting step in such strand-displacement reactions is the endothermic nucleation of a region in which complementary bases are joined[26,28,29] (in this case, the nucleation of hybridization between the F and $\bar{F}$ strands): this

Name	Sequence	
	Domain 1	Domain 2
A	5′ TGCCTTGTAAGAGCGACCAT	CAACCTGGAATGCTTCGGAT 3′
B	5′ GGTCGCTCTTACAAGGCA	CTGGTAACAATCACGGTCTATGCG 3′
C	5′ GGAGTCCTACTGTCTGAACTAACG	ATCCGAAGCATTCCAGGT 3′
F	5′ CGCATAGACCGTGATTGTTACCAG	CGTTAGTTCAGACAGTAGGACTCCTGCTACGA 3′
β	5′ GGTCGCTCTTACAAGGCA	CAGCTAGTTTCACAGTGGCAAGTC 3′
γ	5′ GCAGGCTTCTACATATCTGACGAG	ATCCGAAGCATTCCAGGT 3′
$F_{B\gamma}$	5′ CGCATAGACCGTGATTGTTACCAG	CTCGTCAGATATGTAGAAGCCTGC ACGTCGAT 3′
$F_{C\beta}$	5′ GACTTGCCACTGTGAAACTAGCTG	CGTTAGTTCAGACAGTAGGACTCC TGTCCAGA 3′

Figure 1 Oligonucleotide sequences. Blue and green colouring indicates sections of B and C that hybridize to complementary sections of closing strand F; the red section of F is the overhang at which interaction with opening strand $\bar{F}$ begins. Shorter oligonucleotides corresponding to the domains indicated are used in a control experiment described in the text. Oligonucleotides B1 and C2 used in the control experiment are complementary to domains A1 and A2 respectively of A, including the central four bases that form the hinge, and are therefore two bases longer than the sequences shown above.

is consistent with our observation that the measured second-order rate constants for opening and closing the tweezers are approximately equal.

Dye quenching is used to titrate the closing and removal strands and to determine the state of the machine. The fluorescence intensity drops by a factor of six when the tweezers are closed, back to approximately the same level as from unhybridized, randomly coiled A strands. Figure 3 shows the fluorescence intensity variation as the tweezers are cycled seven times between the open and closed states by successive additions of strands F and $\bar{F}$. The switching time for the machine is approximately 13 s.

To calibrate the motion of the device, we measure the fluorescence intensity as a function of the separation between TET and TAMRA groups. A 24-base oligonucleotide labelled at the 5′ end with TET and a separate 24-mer labelled at the 3′ end with TAMRA are hybridized to complementary sequences at either end of a $(48+n)$-mer ($n = 10, 15, 20, 40$), whose central n-base spacer section is straightened by hybridization to a complementary n-mer. The dye-labelled ends of the two 24-mers are separated only by the spacer section; its length is much less than the persistence length of double-stranded DNA, so it acts as a rigid rod holding the dye groups at a fixed separation. The fluorescence intensity from the open tweezers (an average over many possible open configurations) is equal to the interpolated value for a 17-base spacer: we deduce an approximate average value for the difference in separation between the ends of the tweezers in the open and closed states of 6 nm, corresponding to an angle between the open tweezer arms of 50°.

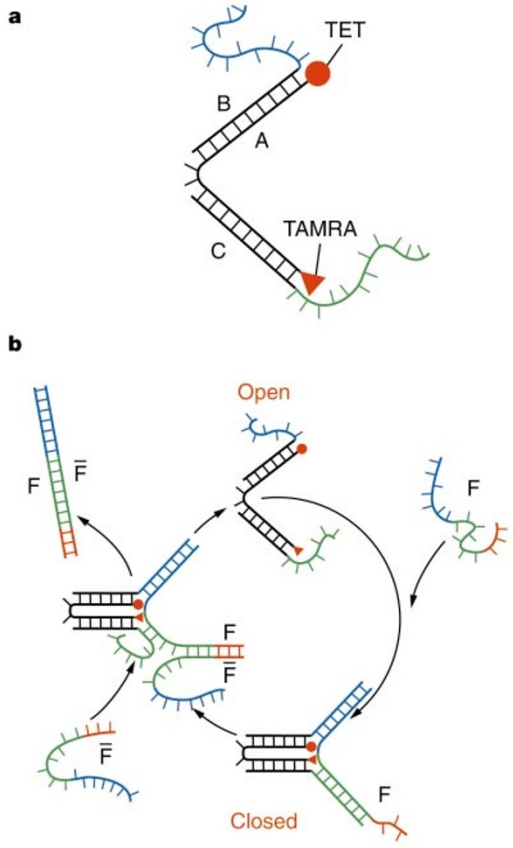

Figure 2 Construction and operation of the molecular tweezers. **a**, Molecular tweezer structure formed by hybridization of oligonucleotide strands A, B and C. **b**, Closing and opening the molecular tweezers. Closing strand F hybridizes with the dangling ends of strands B and C (shown in blue and green) to pull the tweezers closed. Hybridization with the overhang section of F (red) allows $\bar{F}$ strand to remove F from the tweezers, forming a double-stranded waste product F$\bar{F}$ and allowing the tweezers to open. Complementary sections of B, C, F and $\bar{F}$ that hybridize to close and open the tweezers are coloured as in Fig. 1.

As a control we add closing strand F to tweezers which incorporate a modified strand A labelled with TET only: we observe only a 17% drop in the TET fluorescence intensity, five times less than in the case when the other end of the tweezers is labelled with TAMRA. When a fully labelled strand A (incorporating both dye groups) is used but one of the tweezer components B, C is left out, so that the tweezers cannot close, then changes in fluorescence intensity due to successive additions of F and $\bar{F}$ are less than 8% of the change achieved with the complete structure. In contrast, when tweezers are prepared with a fully labelled strand A which is shortened by one or two bases at the 5′ end, changing the position of the point of attachment of the TET group but allowing the tweezers to close normally, we observe quenching ratios of 7.2 and 7.8 respectively on adding F. These experiments indicate that the quenching of TET emission on addition of the closing fuel strand is largely due to the proximity of the TAMRA group in the closed state, and is relatively insensitive to other changes in its environment.

In our model of 'properly closed' tweezers, shown schematically in Fig. 2b, the stiff arms of the tweezers are held together by the closing strand and quenching is due to the proximity of the two dye groups attached to a single strand of DNA. An alternative closed configuration—in which TET emission is also quenched—is a dimer or larger complex (referred to collectively as dimers below) in which closing strands tie the TET group on one strand close to the TAMRA on another (see inset to Fig. 4). To investigate dimer formation, we have made use of modified tweezers made from strands A, β, γ (Fig. 1). Strands β, γ have the same 18-base sequences complementary to A as strands B, C but have different 24-base free ends. Strands $F_{B\gamma}$, $F_{C\beta}$ cannot close either tweezer structure, but can hybridize to link free ends of strands B to those of strand γ, and free ends of strands C to those of strands β, joining one of the original tweezers to one of the modified tweezers to form a dimer.

We have used polyacrylamide gel electrophoresis to compare 'closed tweezers' (A,B,C) + F with 'dimers' (A,B,C) + (A,β,γ) + $F_{B\gamma}$ + $F_{C\beta}$. Figure 4 shows an image of the gel recorded using laser-excited dye fluorescence. Lanes a–e are controls containing incomplete structures; lane l contains dimers. Lanes f–k contain open (f,h,j) and closed (g,i,k) tweezers corresponding to successive additions of closing and removal fuel strands F and $\bar{F}$. Saturated bands in lanes b–f,h,j correspond to structures in which quenching of TET fluorescence is minimum. The dominant 'properly closed' band in the 'closed tweezer' lanes is absent from the 'dimer' lane, consistent with our interpretation that the dominant component of 'closed tweezers' does indeed correspond to 'properly closed' tweezers as designed. Low-intensity bands in the 'closed tweezer' lanes match bands in the 'dimer' lane l, confirming that some dimer formation does occur. To estimate the yield of 'properly closed' tweezers, we measure fluorescence quenching in mixtures of dye-labelled and unlabelled tweezers in which the fraction of TET and TAMRA groups bound together on adding closing fuel strands, and thus the degree of quenching depends on the proportion of 'properly closed' tweezers formed. These controls are described in the Supplementary Information: we estimate that about 80% of tweezers in the experiment recorded in Fig. 3 are 'properly closed' by the closing fuel strand F. We note that dimer formation could in principle be avoided completely by tethering the tweezers to a solid substrate to prevent interaction.

By comparing 'open tweezer' lanes f,h,j in Fig. 4 we deduce that, after each cycle of closing and opening, strand A remains intact and the initial configuration of the open tweezers is recovered. To test whether the duplex structures formed by hydrogen bonding between A, B and A, C survive the forces exerted by hybridization with F in the closed state, we have used an additional strand $\bar{A}$, the complement of A, to test the integrity of the machine by displacing B and C from A. In the absence of other strands, $\bar{A}$ hybridizes with A (producing an eight-fold increase in fluorescence intensity) with a

time to half-completion of 17 s for [A] = [Ā] = 1 μM. When the same concentration of Ā is introduced to ready-formed tweezers in the open state, the time to half-completion for interaction is increased to 4.8×10^3 s by the need for thermally activated displacement of parts of B and C from A before hybridization with Ā can begin. The interaction of Ā with tweezers held in the closed state is an order of magnitude slower than in the open state (time to half-completion, 5×10^4 s); the closed structure inhibits the winding and unwinding of strands that accompanies strand exchange. The high stability of the tweezers, even in the closed state where the hinge region may be strained, indicates that its structural integrity is maintained.

As a further test of our design we checked that the components of the machine interact as intended. We divided each of the strands {A, B, C, F, F̄} into two functionally separate domains, as indicated in Fig. 1. This separation of function may be understood with reference to Fig. 2: domains B1 and B2 of strand B are designed to hybridize with domains A1 and F1, and so on. Polyacrylamide gel electrophoresis at 20 °C (see Methods) of stoichiometric mixtures of all pairs of oligonucleotides from the set {A, B, C, F, F̄, A1 … F̄1, A2 … F̄2} shows that only those pairs that are designed to hybridize do so. This demonstrates that there are no undesired interactions between components of the machine.

A similar structure to that reported here could be used to investigate the interaction between chemically active components attached to the ends of the tweezers or, if combined with a DNA cage[5], to alternately hide and reveal a target group. It is possible to imagine free-running machines using metastable DNA loops as fuel[30]. Because the binding between fuel and machine is sequence-specific, the DNA strands that act as fuel may also serve as information carriers to coordinate components of a complex machine or to carry signals between machines. The use of DNA fuel allows precise control of movements on a nanometre length scale without prodding by a scanning microscope tip; it makes possible coordinated motion of devices which may incorporate elements chosen for their biochemical, optical or electrical properties. Controlled motion provides new opportunities in the design of nanostructures. □

Methods

Oligonucleotides were supplied by Integrated DNA Technologies, Inc.; strand A was purified by high-performance liquid chromatography, other strands were purified by polyacrylamide gel electrophoresis. Stock solutions were prepared by resuspending the lyophilized oligonucleotides in TE buffer (10 mM Tris pH 8.0, 1 mM EDTA) at a nominal 25 μM concentration. Fluorescence quenching was used as an indicator to titrate strands B, C against A and strands F, F̄ against open tweezers (formed of stoichiometric quantities of A, B and C) in SPSC buffer (50 mM Na_2HPO_4 pH 6.5, 1 M NaCl). TET fluorescence was excited with the 514.5-nm line of an argon ion laser (mechanically chopped at 130 Hz), selected by an interference filter with bandpass 10 nm centred at 540 nm and detected by a Si photodiode and phase-sensitive detector. We estimate an error of 10% in determining relative concentrations. Absolute concentrations were obtained from ultraviolet absorption measurements by the commercial supplier of the oligonucleotides; from our measurements of relative concentrations, we estimate that the error in absolute concentrations is of the order of 30%. To form open tweezers 2 μl of stock solution of strand A was diluted to 1 μM using 48 μl SPSC buffer, then stoichiometric quantities of the stock

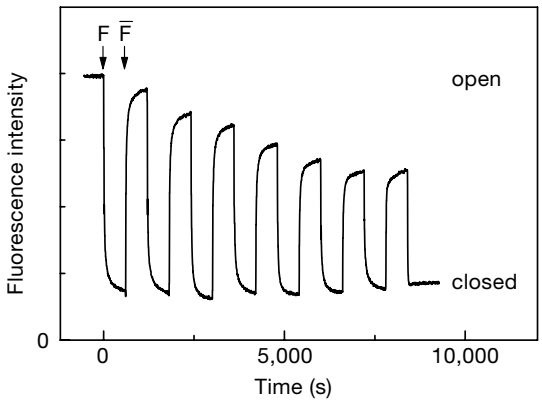

Figure 3 Cycling the molecular tweezers. By adding stoichiometric quantities of closing and removal strands F and F̄ in sequence, the tweezers may be closed and opened repeatedly. When the tweezers are closed, resonant energy transfer from the TET dye to the TAMRA quencher group reduces the fluorescence intensity.

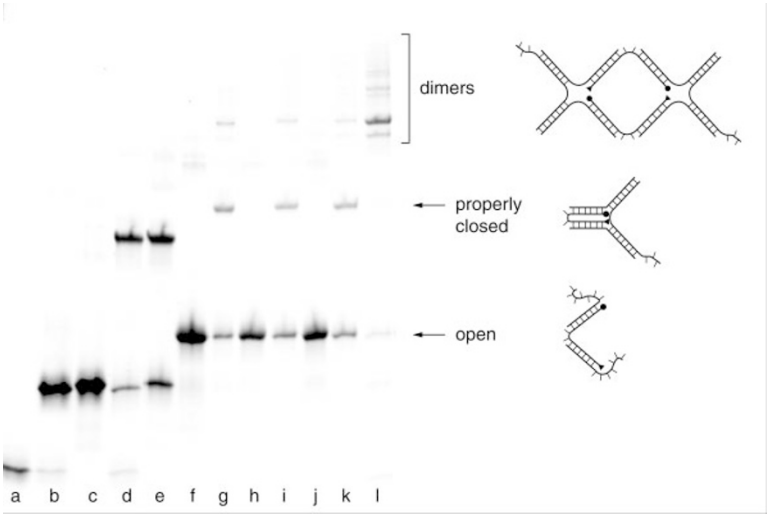

Figure 4 Analysis of tweezer formation by polyacrylamide gel electrophoresis. Lanes as follows: a, strand A; b, A+C; c, A+B; d, A+C+F; e, A+B+F; f, A+B+C (open tweezers); g, (A+B+C)+F (closed tweezers); h–k, two further cycles of opening and closing produced by successive additions of F̄ and F to closed tweezers; l, (A,B,C)+(A,β,γ)+$F_{B\gamma}$+$F_{C\beta}$ (only dimers can form). Schematic structures of open and properly closed tweezers and of a dimer complex are shown next to the appropriate bands.

solutions of strands B and C were added; the mixture was left for >20 min to allow the reaction to reach near-completion. Each addition of a stoichiometric quantity of a stock solution of strand F or $\bar{F}$ resulted in ~3% further dilution of the reactants; after each addition (Fig. 3), reactants were mixed by rapid pipetting up and down lasting <8 s. All measurements were performed at 20 °C.

Polyacrylamide gel electrophoresis (Fig. 4) was performed using a Multiphor II flatbed electrophoresis system with an ExcelGel 48S precast gel (total acrylamide concentration $T = 12.5\%$, bisacrylamide concentration $C = 2\%$; Amersham Pharmacia Biotech). Reactions were performed and 5 μl samples loaded in SPSC buffer with an approximate DNA concentration of 5 μM for each species except $F_{B\gamma}$, $F_{C\beta}$ (2.5 μM). Each reaction was allowed a minimum of 20 min to proceed to near-completion. Fluorescence was excited by the 514.5-nm line of an argon ion laser, selected by an interference filter with bandpass 10 nm centred at 540 nm and recorded by a CCD camera: Fig. 4 is a composite of four images.

Received 12 May; accepted 7 June 2000.

1. Mirkin, C. A., Letsinger, R. L., Mucic, R. C. & Storhoff, J. J. A DNA-based method for rationally assembling nanoparticles into macroscopic materials. *Nature* **382,** 607–609 (1996).
2. Alivisatos, A. P. *et al.* Organization of 'nanocrystal groups' using DNA. *Nature* **382,** 609–611 (1996).
3. Coffer, J. L. *et al.* Dictation of the shape of mesoscale semiconductor nanoparticle assemblies by plasmid DNA. *Appl. Phys. Lett.* **69,** 3851–3853 (1996).
4. Braun, E., Eichen, Y., Sivan, U. & Ben-Yoseph, G. DNA-templated assembly and electrode attachment of a conducting silver wire. *Nature* **391,** 775–778 (1998).
5. Winfree, E., Liu, F., Wenzler, L. A. & Seeman, N. C. Design and self-assembly of two-dimensional DNA crystals. *Nature* **394,** 539–544 (1998).
6. Mao, C., Sun, W. & Seeman, N. C. Assembly of Borromean rings from DNA. *Nature* **386,** 137–138 (1997).
7. Chen, J. & Seeman, N. C. Synthesis from DNA of a group with the connectivity of a cube. *Nature* **350,** 631–633 (1991).
8. Mao, C., Sun, W., Shen, Z. & Seeman, N. C. A nanomechanical device based on the B-Z transition of DNA. *Nature* **397,** 144–146 (1999).
9. Asanuma, H., Ito, T., Yoshida, T., Liang, X. & Komiyama, M. Photoregulation of the formation and dissociation of a DNA duplex by using the *cis-trans* isomerization of azobenzene. *Angew. Chem. Int. Edn Engl.* **38,** 2393–2395 (1999).
10. Porta, H. & Lizardi, P. M. An allosteric hammerhead ribozyme. *Biotechnology* **13,** 161–164 (1995).
11. Tang, J. & Breaker, R. R. Rational design of allosteric ribozymes. *Chem. Biol.* **4,** 453–459 (1997).
12. Araki, M., Okuno, O., Hara, Y. & Sugiura, Y. Allosteric regulation of a ribozyme activity through ligand-induced conformational change. *Nucleic Acids Res.* **26,** 3379–3384 (1998).
13. Robertson, M. P. & Ellington, A. D. *In vitro* selection of an allosteric ribozyme that transduces analytes to amplicons. *Nature Biotechnol.* **17,** 62–66 (1999).
14. Smith, S. B., Finzi, L. & Bustamante, C. Direct mechanical measurements of the elasticity of single DNA groups by using magnetic beads. *Science* **258,** 1122–1126 (1992).
15. Manning, G. S. A procedure for extracting persistence lengths from light-scattering data on intermediate molecular weight DNA. *Biopolymers* **20,** 1751–1755 (1981).
16. Smith, S. B., Yujia, C. & Bustamante, C. Overstretching B-DNA: the elastic response of individual double-stranded and single-stranded DNA groups. *Science* **271,** 795–799 (1996).
17. Stryer, L. & Haugland, R. P. Energy transfer: a spectroscopic ruler. *Proc. Natl Acad. Sci. USA* **58,** 719–726 (1967).
18. Heller, M. J. & Morrison, L. E. in *Rapid Detection and Identification of Infectious Agents* (eds Kingsbury, D. T. & Falkow, S.) 245–256 (Academic, New York, 1985).
19. SantaLucia, J. Jr A unified view of polymer, dumbbell, and oligonucleotide DNA nearest-neighbor thermodynamics. *Proc. Natl Acad. Sci. USA* **95,** 1460–1465 (1998).
20. Record, M. T. Jr, Anderson, C. F. & Lohman, T. M. Thermodynamic analysis of ion effects on the binding and conformational equilibria of proteins and nucleic acids: the roles of ion association or release, screening, and ion effects on water activity. *Q. Rev. Biophys.* **11,** 103–178 (1978).
21. Bockelmann, U., Essevaz-Roulet, B. & Heslot, F. Molecular stick-slip motion revealed by opening DNA with piconewton forces. *Phys. Rev. Lett.* **79,** 4489–4492 (1997).
22. Svoboda, K., Schmidt, C. F., Schnapp, B. J. & Block, S. M. Direct observation of kinesin stepping by optical trapping interferometry. *Nature* **365,** 721–727 (1993).
23. Kuo, S. C. & Sheetz, M. P. Force of single kinesin groups measured with optical tweezers. *Science* **260,** 232–234 (1993).
24. Finer, J. T., Simmons, R. M. & Spudich, J. A. Single myosin group mechanics: piconewton forces and nanometre steps. *Nature* **368,** 113–119 (1994).
25. Ishijima, A. *et al.* Single-group analysis of the actomyosin motor using nano-manipulation. *Biochem. Biophys. Res. Commun.* **199,** 1057–1063 (1994).
26. Green, C. & Tibbetts, C. Reassociation rate limited displacement of DNA strands by branch migration. *Nucleic Acids Res.* **9,** 1905–1918 (1981).
27. Lee, C. S., Davis, R. W. & Davidson, N. A physical study by electron microscopy of the terminally repetitious, circularly permuted DNA from the coliphage particles of *Escherichia coli* 15. *J. Mol. Biol.* **48,** 1–22 (1970).
28. Wetmur, J. G. & Davidson, N. Kinetics of renaturation of DNA. *J. Mol. Biol.* **31,** 349–370 (1968).
29. Radding, C. M., Beattie, K. L., Holloman, W. K. & Wiegand, R. C. Uptake of homologous single-stranded fragments by superhelical DNA: IV branch migration. *J. Mol. Biol.* **116,** 825–839 (1977).
30. Turberfield, A. J., Yurke, B. & Mills, A. P. Jr Coded self-assembly of DNA nanostructures. *Bull. Am. Phys. Soc.* **44,** 1711 (1999).

Supplementary information is available on *Nature*'s World-Wide Web site (http://www.nature.com) or as paper copy from the London editorial office of *Nature*.

Acknowledgements

F.C.S. thanks the Alexander von Humboldt Foundation for support.

Correspondence and requests for materials should be addressed to B.Y. (e-mail: yurke@lucent.com) or A.J.T. (e-mail: a.turberfield@physics.ox.ac.uk).

Influencing intramolecular motion with an alternating electric field

Veronica Bermudez*, Nathalie Capron†, Torsten Gase*, Francesco G. Gatti‡, François Kajzar*, David A. Leigh‡, Francesco Zerbetto† & Songwei Zhang‡

** LETI (CEA - Technologies Avancées), DEIN/SPE/GCO, CE Saclay, 91191 Gif-sur-Yvette Cedex, France*
† Dipartimento di Chimica "G. Ciamician", Università degli Studi di Bologna, V. F. Selmi 2, 40126, Bologna, Italy
‡ Centre for Supramolecular and Macromolecular Chemistry, Department of Chemistry, University of Warwick, Coventry CV4 7AL, UK

Analogues of mechanical devices that operate on the molecular level[1–5], such as shuttles[6–10], brakes[11], ratchets[12,13], turnstiles[14] and unidirectional spinning motors[15,16], are current targets of both synthetic chemistry and nanotechnology. These structures are designed to restrict the degrees of freedom of submolecular components such that they can only move with respect to each other in a predetermined manner, ideally under the influence of some external stimuli. Alternating-current (a.c.) electric fields are commonly used to probe electronic structure, but can also change the orientation of molecules[17–19] (a phenomenon exploited in liquid crystal displays), or interact with large-scale molecular motions, such as the backbone fluctuations of semi-rigid polymers[20,21]. Here we show that modest a.c. fields can be used to monitor and influence the relative motion within certain rotaxanes[22], molecules comprising a ring that rotates around a linear 'thread' carrying bulky 'stoppers' at each end. We observe strong birefringence at frequencies that correspond to the rate at which the molecular ring pirouettes about the thread, with the frequency of maximum birefringence, and by inference also the rate of ring pirouetting giving rise to it, changing as the electric field strength is varied. Computer simulations and nuclear magnetic resonance spectroscopy show the ring rotation to be the only dynamic process occurring on a timescale corresponding to the frequency of maximum birefringence, thus confirming that mechanical motion within the rotaxanes can be addressed, and to some extent controlled, by oscillating electric fields.

During routine investigations of the influence of discrete large-amplitude internal molecular motions on optical properties, an a.c. electric field was used to address the structures of two hydrogen-bond-assembled rotaxanes, **1** and **2**, and their uninterlocked molecular fragments. The rotaxanes differ from each other only in the nature of the thread; **1** contains two nitrone hydrogen-bond acceptors, and **2** a fumaramide unit (Fig. 1). Both threads template the formation of the benzylic amide macrocycle about them to form [2]rotaxanes in yields of 70 and 97%, respectively[23].

The a.c. field effects on **1** and **2** in dioxane (the nonpolar, non-electrically-conducting solvent of choice for such experiments[24]) were monitored by the quadratic dependence of the refractive index, that is, by recording the electro-optic Kerr effect. (Put simply, the light travelling through a sample undergoes a time-independent phase shift accompanied, in an a.c. field, by a time-dependent phase shift of twice that frequency.) Figure 2a shows the experimentally determined Kerr constant for the two rotaxanes as a function of frequency. A major response was somewhat unexpectedly discovered for both rotaxanes at values close to 50 Hz at 0.35 V μm^{-1}—an unusual frequency which cannot easily be attributed to any intrinsic electronic phenomenon. Signals in this frequency range are absent for the corresponding uninterlocked components, that is, the threads or macrocycle alone, or the solvent itself, indicating that the response is intrinsically related to the mechanically interlocked architecture of the rotaxanes. Concentration-dependent measure-